Appl Nanosci (2016) 6:235–241
DOI 10.1007/s13204-015-0425-7

ORIGINAL ARTICLE

Formation of Al-doped ZnO thin films on glass by sol–gel process and characterization

M. U. Shahid[1] · K. M. Deen[2] · A. Ahmad[1] · M. A. Akram[3] · M. Aslam[4] · W. Akhtar[1]

Received: 2 January 2015 / Accepted: 4 March 2015 / Published online: 17 March 2015

Abstract In this study, pure ZnO and Al-doped ZnO thin films were developed on glass by sol–gel process followed by drying and annealing in air at 170 and 400 °C, respectively. The surface morphology and structural characteristics were determined through scanning electron microscopy, atomic force microscopy and X-ray diffraction. The Fourier transform infrared spectroscopy validated the formation of Al-doped ZnO film on glass substrate. It was evaluated that 1 at% aluminum (Al) doping in ZnO film showed low electrical resistivity and higher charge carrier concentration due to uniformly dispersed regular shape crystallites as compared to pure ZnO and 2 at% 'Al'-doped thin films.

Keywords Thin film · Resistivity · Carrier concentration · Glass · Sol–gel

✉ M. U. Shahid
engr.umairshahid@live.com

[1] Department of Metallurgical and Materials Engineering, University of Engineering and Technology, Lahore 54890, Pakistan

[2] Department of Metallurgy and Materials Engineering, CEET, University of the Punjab, Lahore 54590, Pakistan

[3] School of Chemical and Materials Engineering, National University of Sciences and Technology, Islamabad 44000, Pakistan

[4] Mechanical Engineering Department, University Tecknologi Petronas, 31750 Seri Iskandar, Malaysia

Introduction

The transparent conducting thin films have great importance in the electrical and optical devices, i.e., flat panel display and dye-sensitized solar cells. The thin films are usually composed of semiconducting metal oxide with doping of trivalent or pentavalent element for the development of higher electrical conductivity (Chopra et al. 1983).

At the start of twentieth century, Badeker (1907) developed good electrically conductive transparent cadmium oxide thin film by sputtering and thermal oxidation of cadmium on glass. From last three decades, indium-doped tin oxide, indium oxide and zinc oxide transparent conducting films have been established. But their performance have been limited in solar cells due to their high electrical resistivity and lower mobility of charge carriers (Coutts et al. 2000).

Indium-doped tin oxide (ITO) thin films are highly transparent and have good electrical conductivity. But these films are expensive due to doping of rare earth indium and low stability in hydrogen plasma. The deposition of zinc oxide-based thin films on glass is capable of replacing expensive ITO films. These films have considerable electrical conductivity, optical transparency, low cost, non-toxicity and good stability to plasma environment. However, the intrinsic semiconductive characteristics of ZnO could not compete with the performance efficiency of ITO films. The conductivity of ZnO transparent film could be enhanced by optimizing doping level and processing parameters. In this way, ZnO thin films would be an attractive alternative to replace ITO for some promising applications such as solar cells, transducers, gas sensors and heating mirrors (Kim and Tai 2007; Wu 2010).

In the last decade, the extrinsic ZnO-based thin films doped with various elements, i.e., aluminum (Al), indium

(In), tin (Sn), gallium (Ga) and manganese (Mn) have been developed (Hao et al. 2002; Lee and Park 2003; Chen et al. 2007). Beside other doping elements, the change in atomic concentration of 'Al' in ZnO can influence the crystallite size and film thickness (Lee and Park 2003). Salam et al. (2013) also reported that resistivity of intrinsic ZnO thin films can be decreased by doping 'Al' up to 1 at%.

Various methods of ZnO deposition on glass have been adopted, i.e., plasma jet (Hsu et al. 2011; chemical vapor deposition Polley et al. 1999; spray pyrolysis Sahay and Nath 2008; magnetron sputtering Ruske et al. 2008; Wu 2010; thermal degradation of hydrogels (Tredici et al. 2011) and sol–gel process; however, sputtering is the widely utilized method for ZnO thin film deposition to achieve good electrical and optical properties at low temperature. But this method is expensive and has low deposition rate. Sol–gel process is getting much attention because of its simplicity and low cost. This process is capable of producing high-quality coatings even on both large- and small-sized substrates which can be employed for advanced applications (Silva and Darbello Zaniquelli 1999; Lee and Park 2003; Ng et al. 2012).

In sol–gel process, the significant factors which affect the characteristics of conductive oxide films are chemical composition of sol, pH, substrate/film interaction, viscosity and coating technique (dip or spin). After the deposition process, furnace atmosphere, drying and annealing time are important factors (Silva and Darbello Zaniquelli 1999).

In previous studies, it has been proved that high annealing temperature is needed to get lower resistivity as Lee and Park (2003) reported. However, in the current research work, Al-doped ZnO thin films were developed at lower annealing temperature 400 °C and have achieved extensive results. The effect of 'Al' doping level on film morphology, structure and electrical properties was investigated by scanning electron microscopy (SEM), atomic force microscopy (AFM), X-ray diffraction (XRD), Fourier transform infrared spectroscopy (FTIR) and Hall effect measurments.

Experimental setup

Soda lime glass slides having dimensions (25 mm × 75 mm × 1 mm) were selected as a substrate material. Before deposition, slides were sequentially washed with acetone, 2-propanol and deionized water to remove any dirt, oil or grease. The 0.6 M sol solution containing zinc acetate di-hydrate in 2-propanol was prepared by using magnetic stirrer for 60 min at 70 °C. The solution became turbid immediately, and di-ethanolamine (DEA) was then added drop wise to stabilize sol solution by adjusting molar ratio of Zn^{+2}/DEA equal to unity. Three types of sol solutions, one without aluminum (designated as ZnO) and two with 1 (AZO-1) and 2 at% 'Al' (AZO-2) concentration, were prepared by adding calculated amount of hydrated aluminum nitrate. The aging was done by keeping these sol solutions in airtight bottles for 1 week at room temperature.

Aged sol solutions were deposited on pre-cleaned glass slides by dip coating process. The withdrawal speed of glass slides was kept 6 cm/min followed by drying on hot plate at 170 °C for 10 min. The coating and drying cycle was repeated thrice, and the samples were annealed in a furnace at 400 °C with a heating rate of 1.5 °C/min for 1 h.

The surface morphology of ZnO, AZO-1 and AZO-2 thin films was analyzed by SEM (JEOL JSM6490A) and AFM (JSPM5200). XRD (PHILIPS-binary scan) patterns were obtained using Cu-K_α radiations source operated at 40 kV and 30 mA for structural evaluation. FTIR was also performed to validate the formation of ZnO-based thin films. Films thickness was calculated by Profilometer model NANOVEA CCS-PRIMA with chromatic confocal sensor. The electrical characteristics of these films were investigated by utilizing Van der Pauw variable temperature Hall effect measurement system (Ecopia HMS 5000). The Hall effect is actually phenomenon in which magnetic field is applied perpendicular to the direction of the motion of charge carriers and then it exerts the force which is also perpendicular to the direction of the motion of charges and magnetic field itself. As shown in Fig. 1, consider parallelepiped-shaped specimen having its one corner at the origin of the coordinate system, and in the influence of the electric field, current travels in the

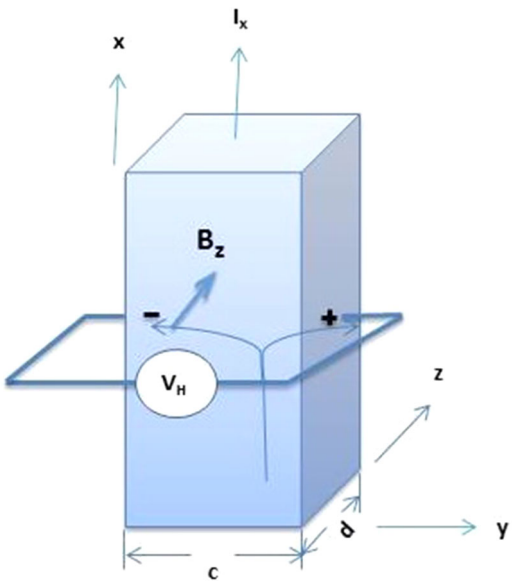

Fig. 1 Schematic demonstration of Hall effect. Current I_x generates positive and negative charges carriers that are deflected by magnetic field B_z and give rise to Hall voltage, V_H

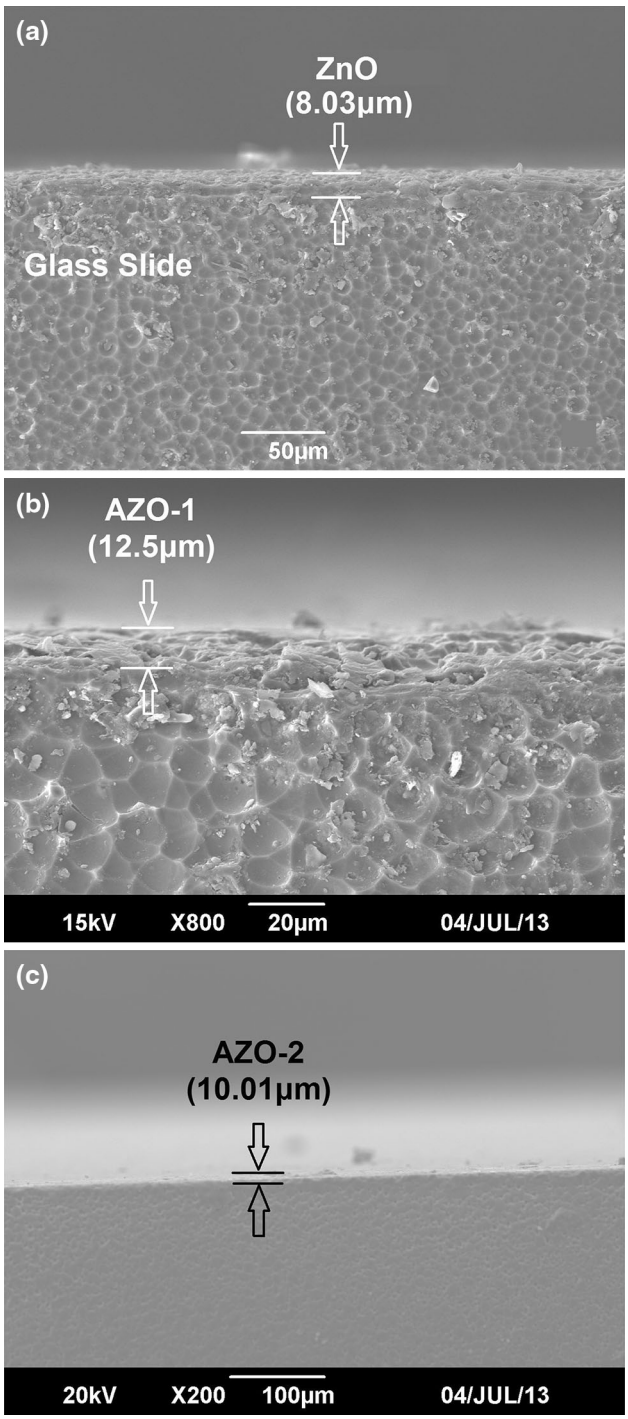

Fig. 2 Cross-sectional view of glass substrate to evaluate film thickness **a** ZnO, **b** AZO-1, and **c** AZO-2

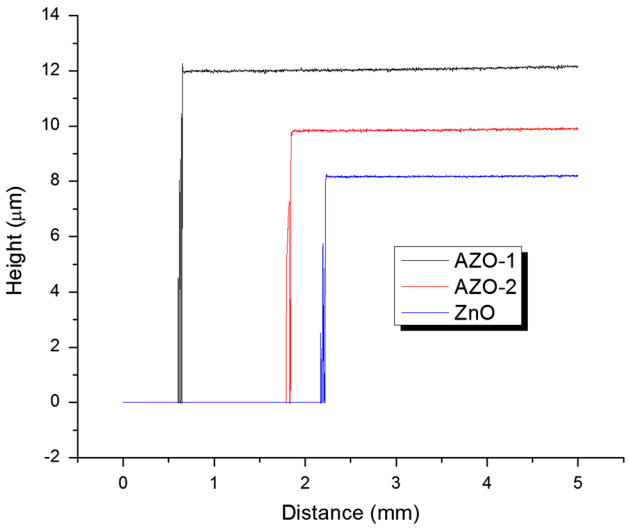

Fig. 3 Films thickness of ZnO, AZO-1 and AZO-2 measured by profilometer

x direction. Now if the magnetic field is applied in the z (denoted by B_z) direction, then due to its influence, charge carriers experience magnetic force so negatively charged particles deflected toward left side while positive toward right side; in this way, maximum electric potential is generated between two boundaries of the specimen in y direction, and this voltage is called Hall voltage V_H (Calister 2007).

The magnitude of Hall voltage depends upon current I_x, magnetic field B_z and thickness d of specimen or thin conducting films. It is computed from the equation given below

$$V_H = \frac{R_H I_x B_z}{d} \quad (1)$$

where R_H is the Hall coefficient; its value depends upon the nature of the materials.

Results and discussions

The average film thickness of ZnO, AZO-1 and AZO-2 thin films was measured as shown in Fig. 2 and validated by profilometer as shown in Fig. 3. All glass samples were deposited with ZnO and Al-doped ZnO thin films under similar conditions besides varying aluminum doping level. The significant difference in thickness was observed by varying aluminum content in sol solution. AZO-1 film with 1 % Al doping was found to have maximum thickness (12.5 μm) than simple ZnO and AZO-2. These have average thickness of 8.03 and 10.01 μm, respectively. It was also evaluated that after first dipping and drying cycle, the film structure was porous and had uneven surface thickness. The successive second and third dipping cycles eliminated pores and defects due to penetration of sol solution, hence making the film more compact and uniform. The topographical images by AFM validated the formation of elongated ZnO crystals tangled with each other, whereas upon 1 at% aluminum doping in ZnO, the

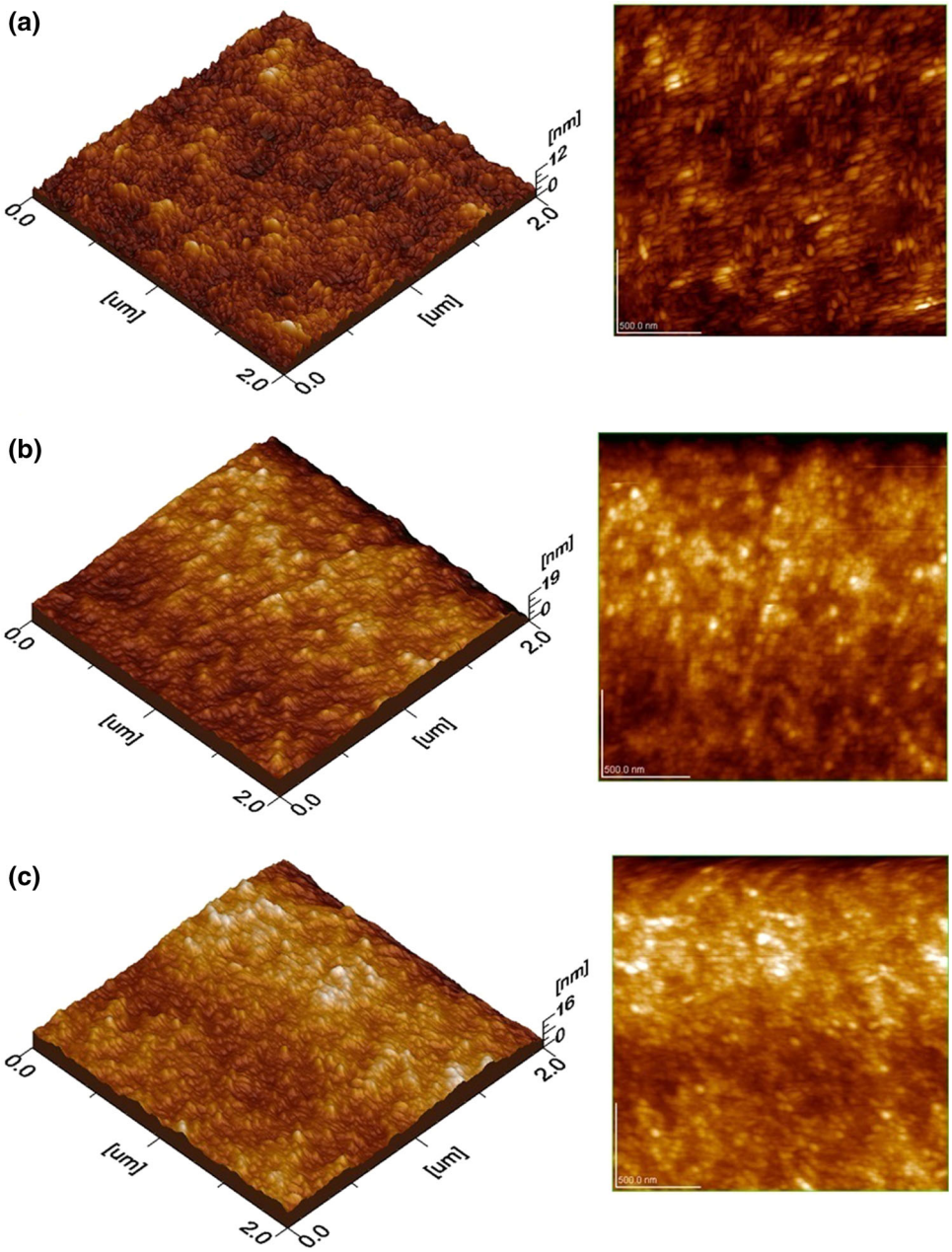

Fig. 4 Surface topography and morphology of thin films by AFM **a** ZnO, **b** AZO-1, and **c** AZO-2

film formed was more compact, uniform and dense as shown in Fig. 4a and b, respectively. It was also observed that the shape of aluminum-doped crystallites within the thin film was more regular and spherical. The surface roughness (RMS) of ZnO films was higher and variable compared to AZO-1 which was relatively more smooth. Figure 4c represents higher aluminum content (2 at% Al) in AZO-2, and the shape of crystallites was distorted having less random orientation. In AZO-2, the Al^{3+} ions substitution within the crystal lattice of ZnO was restricted due to limited solubility of Al^{3+} ions. The saturation of Al^{3+} in the crystallites of AZO-2 film also distorted the shape. In addition to the crystallite distortion, the Al_2O_3 precipitates segregation was also observed at the grain boundaries of crystallites. These results were in support to the findings of Salam et al. (2013) who described that low concentration of 'Al' provided nucleation sites and produced refined thin films. Figure 5 shows the variation in film thickness and root mean square (RMS) roughness of ZnO and AZO films as a function of Al doping level. It was seen that 1 at% Al doping produced maximum film thickness (12.5 nm) with lower RMS (1.31 nm) compared to ZnO and AZO-2 which have 8.02 and 10.10 nm film thickness, respectively.

The XRD patterns of ZnO, AZO-1 and AZO-2 specimens are represented in Fig. 6. XRD signatures were

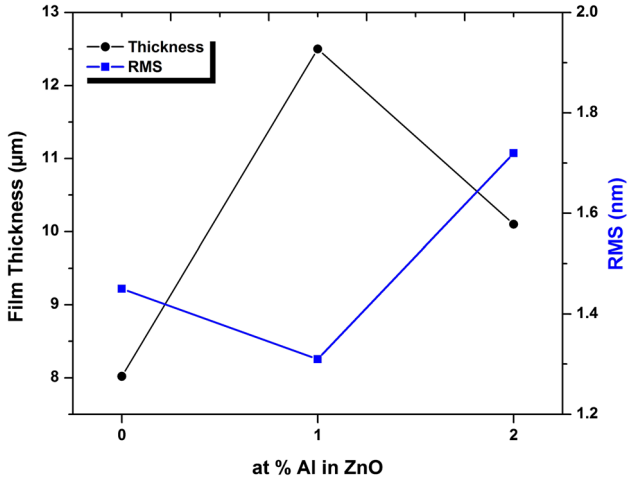

Fig. 5 Film thickness and RMS of as a function of Al doping level

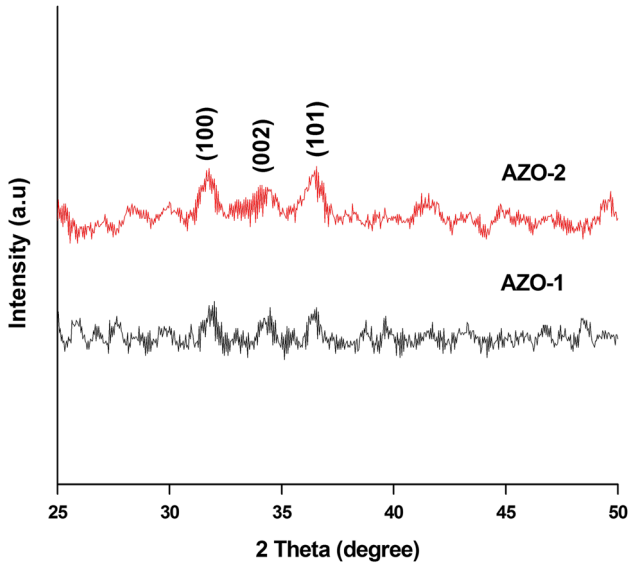

Fig. 6 XRD patterns of AZO-1 and AZO-2 thin films

analyzed using X'pert high score and validated to (JCPDS 36-1451) wurtzite; neither aluminum nor alumina phases in doped thin oxide films were detected. The absence of these phases indicated the possibility of substitutional replacement of Zn^{2+} by Al^{3+} in wurtzite crystal lattice. The major diffraction of ZnO was originated from (100), (002) and (101) planes. The films which are usually annealed above 500 °C exhibit preferred growth orientation along (002) plane (Tang and Cameron 1994; Musat et al. 2004). The drop in intensity at (002) plane in AZO-2 film was considered due to crystal lattice distortion by excess Al^{3+} ions precipitation form in ZnO. (Sengupta et al. 2012) also reported that the shift of diffraction from (002) to (001) and (101) planes was due to increased concentration of 'Al' in 'ZnO' beyond the solubility limit.

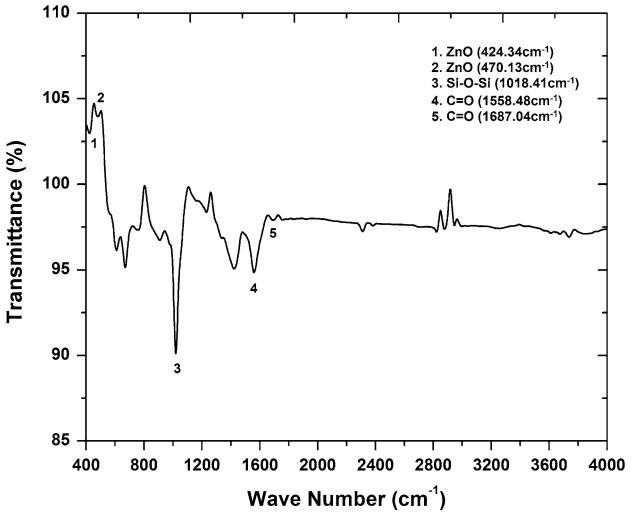

Fig. 7 FTIR spectrum of AZO-1 thin film showing characteristics transmittance and absorption peaks of Zn–O, Al–O and Si–O–Si bonds

The crystallite size was calculated from Scherer's Eq. 1 as follows

$$t = \frac{0.94\lambda}{\beta_{1/2}}\mathrm{Cos}\theta \qquad (2)$$

where 'λ' is the wavelength of Cu-Kα_1 (0.15394 nm), and '$\beta_{1/2}$' is the full width at half maximum (FWHM) by XRD peak at (002) plane. The average crystallite size of AZO-1 and AZO-2 was 13.803 and 18.411 nm, respectively. The increase in 'Al' concentration from 1 to 2 at% distorted the crystallite shape as shown in Fig. 4b and c, and it was validated quantitatively by increase in crystallite size from XRD data. It was also investigated that with 1 at% doping of aluminum, the crystal lattice of ZnO was saturated and due to the large atomic radii of 'Al,' the lattice strain was relatively higher in AZO-1 (8.84×10^{-3}) than AZO-2 (6.60×10^{-3}).

The FTIR spectroscopy was used to validate the formation of 'Al'-doped ZnO thin film as shown in Fig. 7. The spectrum of AZO-1 was compared to pure ZnO thin films as discussed by Ivanova et al. (2010). The relative positions of IR bands depend on chemical composition and morphology of crystallites within the film. Two small bands at 424.34 and 470.13 cm^{-1} corresponded to the vibrations of Zn–O stretching bonds. The broad absorption band within wave number (497.63–594.07 cm^{-1}) represented the bending of Al–O bond, and sharp band at 1018.41 cm^{-1} was attributed to the base glass Si–O–Si bonds. The absorption signatures at 1558.48 and 1687 cm^{-1} were originated due to symmetric and asymmetric vibrations of C=O bond, respectively. Beyond 1764.86 cm^{-1}, no sharp absorption peak was observed and AZO-1 thin film on glass showed 95–97.5 % transmittance

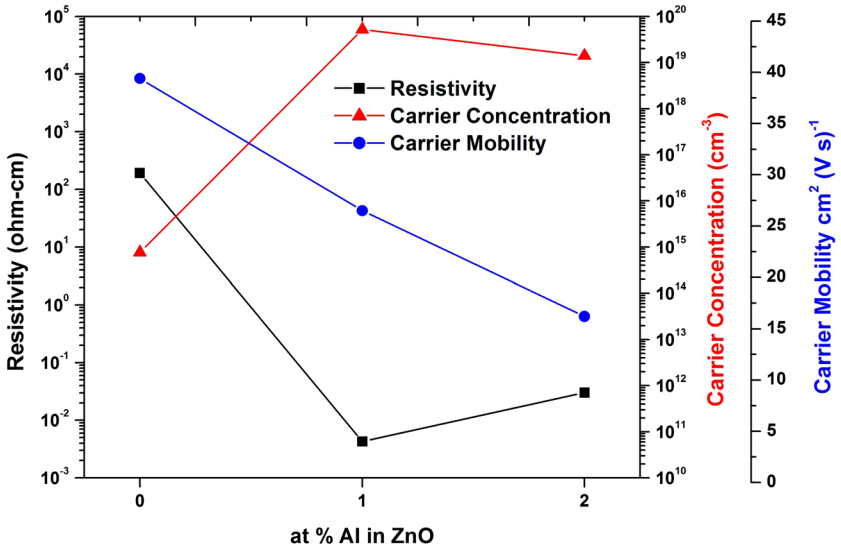

Fig. 8 Electrical characteristics of intrinsic ZnO, AZO-1 and AZO-2 thin films

in the infrared regime (Khan et al. 2011; Djouadi et al. 2012).

Electrical resistivity of AZO thin films largely depends on charge carrier concentration which in turn depends on the degree of substitution of 'Zn' by 'Al' and amount of oxygen vacancies in the crystal lattice of ZnO. Substitution of 'Al' on Zinc site within crystal lattice could increase the charge carrier concentration and could reduce the electrical resistivity of thin film (Wu 2010). As shown in Fig. 8, the electrical resistivity of intrinsic ZnO films was 1.92×10^2 Ω cm and with 'Al' doping, the films exhibited lower electrical resistivity. The doping of 'Al' increased the charge carrier concentration due to difference in the transition states of Zn^{2+} and Al^{3+} ions in the crystal lattice. The lowest electrical resistivity (4.27×10^{-3} Ω cm) with maximum charge carrier concentration (5.21×10^{19} cm^{-3}) was achieved in AZO-1 thin film. It was also evident that charge carrier mobility decreased from 39.4 to 16.2 cm^2 - V^{-1} s^{-1} in AZO-1 thin film than ZnO. When doping level of 'Al' was increased to 2 at% in AZO-2 thin film, the resistivity again rose to 3.01×10^{-2} Ω cm. This increase in resistivity was corresponded to the distortion of crystallites in AZO-2 film. The limited solubility of 'Al' in ZnO lattice beyond 1 at% resulted in the precipitation of Al_2O_3 at grains boundaries. These precipitates were formed due to oxidation of 'Al' during drying and subsequent annealing. This fact was in support to Zhou et al. (2007) who reported that ZnO-based thin films at low concentrations (below 1 at%) of 'Al' give good conductivity and beyond it may produce detrimental effects on electrical properties. The segregation of Al_2O_3 at crystallite grain boundaries could hinder charge transportation within the film. The highest electrical resistivity in ZnO film was obtained due to anisotropic behavior of elongated ZnO crystallites and their non-uniform distribution within the film structure.

Conclusion

It was deduced that aluminum doping in ZnO thin films greatly affects the crystallite morphology in the thin films. The doping of 'Al' up to 1 at% produced more regular-shaped crystallites by sol–gel process. The lowest electrical resistivity (4.27×10^{-3} Ω cm) and higher carrier concentration (5.21×10^{19} cm^{-3}) were achieved in 1 at% 'Al' doping (AZO-1) in ZnO. The high resistivity and low charge carrier concentration in pure ZnO and 2 at% 'Al'-doped films were attributed to the formation of Al_2O_3 precipitates and anisotropic behavior of elongated crystallites.

Acknowledgments This work has been supported by University of Engineering and Technology, Lahore, National University of Sciences and Technology, Islamabad, and University of the Punjab, Lahore.

References

Badeker K (1907) Electrical conductivity and thermo-electromotive force of some metallic compounds. Ann Phys 22:749–766

Callister WD, Rethwisch DG (2007) Materials science and engineering: an introduction, vol 7. Wiley, New York

Chen W et al (2007) Influence of doping concentration on the properties of ZnO: Mn thin films by sol–gel method. Vacuum 81(7):894–898

Chopra KL et al (1983) Transparent conductors—a status review. Thin Solid Films 102(1):1–46

Coutts TJ et al (2000) Search for improved transparent conducting oxides: A fundamental investigation of CdO, Cd_2SnO_4, and Zn_2SnO_4. J Vac Sci Technol A 18(6):2646–2660

Djouadi D et al (2012) Amplification of the UV emission of ZnO: Al thin films prepared by sol–gel method. J Mater Environ Sci 3(3):585–590

Hao X et al (2002) Retracted: thickness dependence of structural, optical and electrical properties of ZnO: Al films prepared on flexible substrates. Appl Surf Sci 189(1–2):18–23

Hsu Y-W et al (2011) Deposition of zinc oxide thin films by an atmospheric pressure plasma jet. Thin Solid Films 519(10):3095–3099

Ivanova T et al (2010) Study of ZnO sol–gel films: Effect of annealing. Mater Lett 64(10):1147–1149

Khan ZR et al (2011) Optical and structural properties of ZnO thin films fabricated by sol–gel method. Mater Sci Appl 02(05):340–345

Kim Y-S, Tai W-P (2007) Electrical and optical properties of Al-doped ZnO thin films by sol–gel process. Appl Surf Sci 253(11):4911–4916

Lee J-H, Park B-O (2003) Transparent conducting ZnO: Al, In and Sn thin films deposited by the sol–gel method. Thin Solid Films 426(1):94–99

Musat V et al (2004) Al-doped ZnO thin films by sol–gel method. Surf Coat Technol 180–181:659–662

Ng Z-N et al (2012) Effects of annealing temperature on ZnO and AZO films prepared by sol–gel technique. Appl Surf Sci 258(24):9604–9609

Polley TA et al (1999) Deposition of zinc oxide thin films by combustion CVD. Thin Solid Films 357(2):132–136

Ruske F et al (2008) Reactive deposition of aluminium-doped zinc oxide thin films using high power pulsed magnetron sputtering. Thin Solid Films 516(14):4472–4477

Sahay PP, Nath RK (2008) Al-doped zinc oxide thin films for liquid petroleum gas (LPG) sensors. Sens Actuator B Chem 133(1):222–227

Salam S et al (2013) Sol–gel synthesis of intrinsic and aluminum-doped zinc oxide thin films as transparent conducting oxides for thin film solar cells. Thin Solid Films 529:242–247

Sengupta J et al (2012) Effect of annealing on the structural, topographical and optical properties of sol–gel derived ZnO and AZO thin films. Mater Lett 83:84–87

Silva RF, Darbello Zaniquelli ME (1999) Aluminium doped zinc oxide films: formation process and optical properties. J Non Cryst Solids 247(1–3):248–253

Tang W, Cameron DC (1994) Aluminum-doped zinc oxide transparent conductors deposited by the sol–gel process. Thin Solid Films 238(1):83–87

Tredici IG et al (2011) Micropatterned nanocrystalline zinc oxide thin films obtained through metal-loaded hydrogels. Thin Solid Films 519(18):5854–5860

Wu GM, Chen YF, Lu HC (2011) Aluminum-doped zinc oxide thin films prepared by sol-gel and RF magnetron sputtering. Acta Phys Pol A 120(1):1–149

Zhou H-M et al (2007) Preparation of aluminum doped zinc oxide films and the study of their microstructure, electrical and optical properties. Thin Solid Films 515(17):6909–6914